

## Supplementary Information

### **Zeta-carbonic anhydrases show CS<sub>2</sub> hydrolase activity: a new metabolic carbon acquisition pathway in diatoms?**

Vincenzo Alterio,<sup>‡,†</sup> Emma Langella,<sup>‡,†</sup> Martina Buonanno,<sup>‡</sup> Davide Esposito,<sup>‡</sup> Alessio Nocentini,<sup>§</sup> Emanuela Berrino,<sup>§</sup> Silvia Bua,<sup>§</sup> Maurizio Polentarutti,<sup>⊥</sup> Claudiu T. Supuran,<sup>§</sup> Simona Maria Monti<sup>‡,\*</sup> and Giuseppina De Simone<sup>‡,\*</sup>

<sup>‡</sup> Istituto di Biostrutture e Bioimmagini-CNR, via Mezzocannone 16, 80134 Napoli, Italy

<sup>§</sup> NEUROFARBA Department, Pharmaceutical and Nutraceutical Section, University of Firenze, Via Ugo Schiff 6, 50019 Sesto Fiorentino, Italy

<sup>⊥</sup>Elettra - Sincrotrone Trieste, s.s. 14 Km 163.5 in Area Science Park, Basovizza (Trieste) 34149, Trieste, Italy.

<sup>†</sup>These authors contributed equally to the work

Correspondence authors. Phone: Tel: +39-081-2534583, E-mail: marmonti@unina.it (SMM) or +39-081-2534579; E-mail: giuseppina.desimone@cnr.it (GDS).

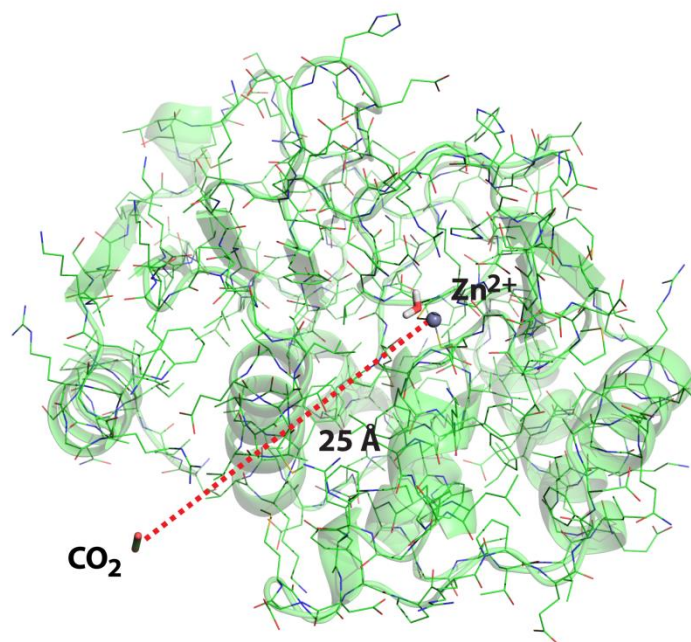


**Figure S1.** Starting configuration for simulations B1-B3. CO<sub>2</sub> molecule (stick representation) is placed out of the enzyme at ~ 5 Å from tunnel entrance and 25 Å from zinc ion (grey sphere). Distance between CO<sub>2</sub> and Zn<sup>2+</sup> is shown as a red dashed line. Protein residues are also displayed.

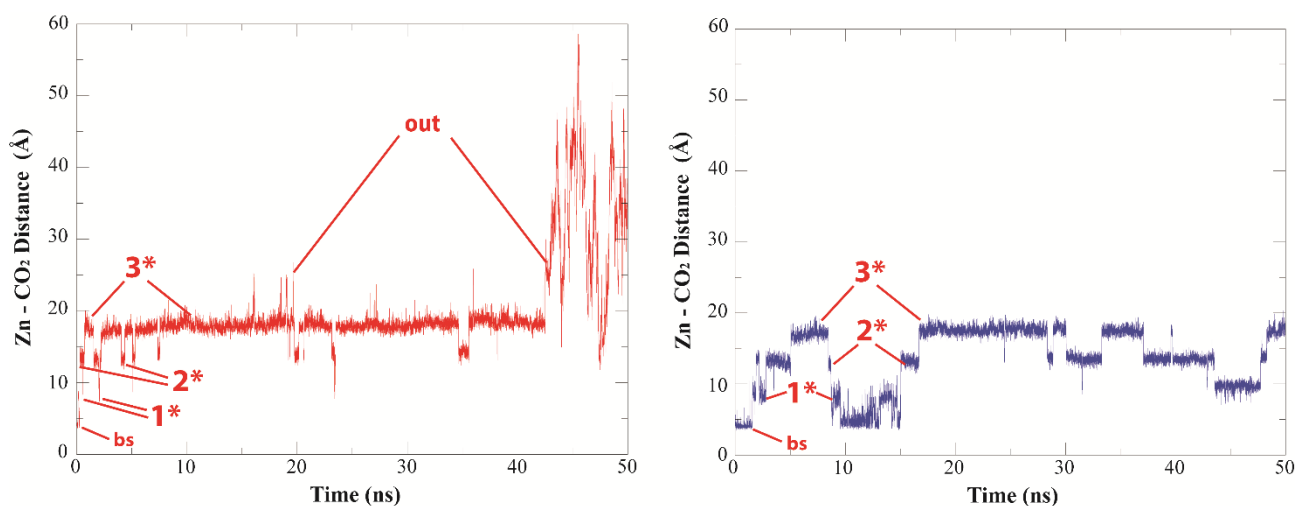


**Figure S2.** Distance between the Zn<sup>2+</sup> ion and the CO<sub>2</sub> carbon atom plotted as a function of time for A2 (red, left panel) and A3 (blue, right panel) trajectories. Pockets (**1\***, **2\***, **3\***) corresponding to CO<sub>2</sub> positions are indicated. **bs** corresponds to CO<sub>2</sub> position in its binding site, according to the crystallographic structure.

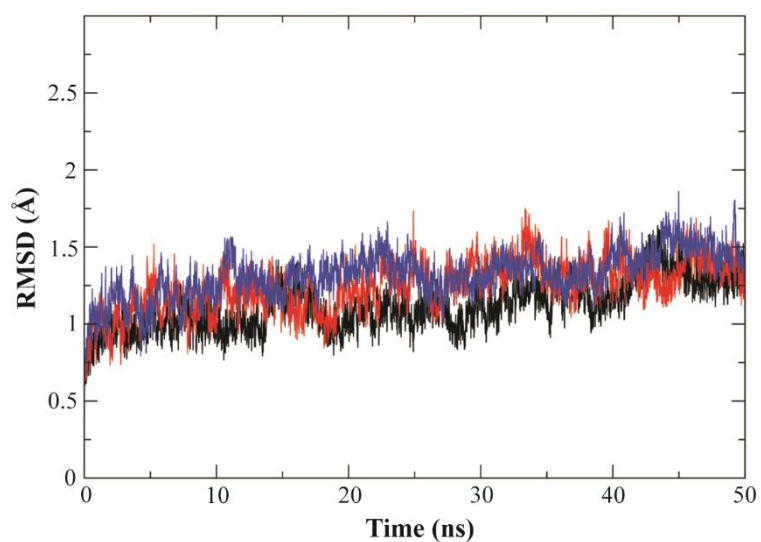


**Figure S3.** Root-Mean-Square Deviation (RMSD) computed on  $C\alpha$  atoms as a function of time for A1 (black), A2 (red) and A3 (blue) trajectories. RMSD indicates the stability of protein structure during simulation time.

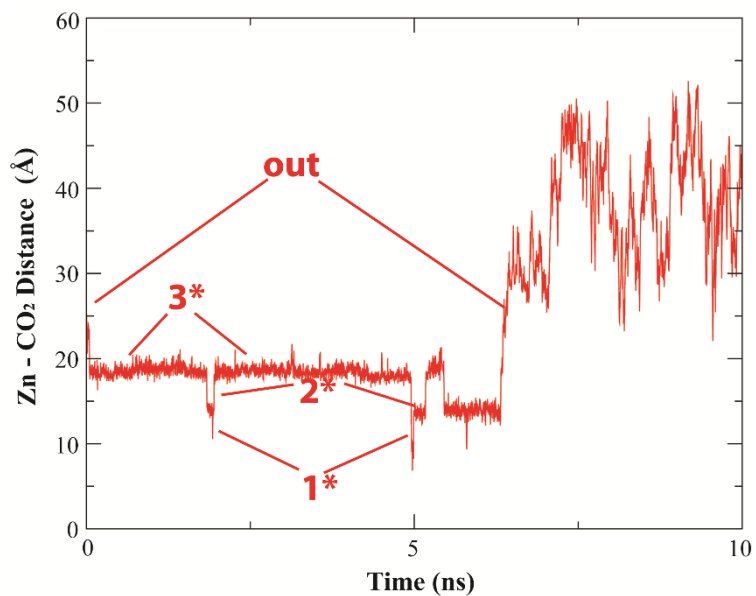


**Figure S4.** Distance between the Zn<sup>2+</sup> ion and the CO<sub>2</sub> carbon atom plotted as a function of time for B2 trajectory. Pockets (1\*, 2\*, 3\*) corresponding to CO<sub>2</sub> positions are indicated.

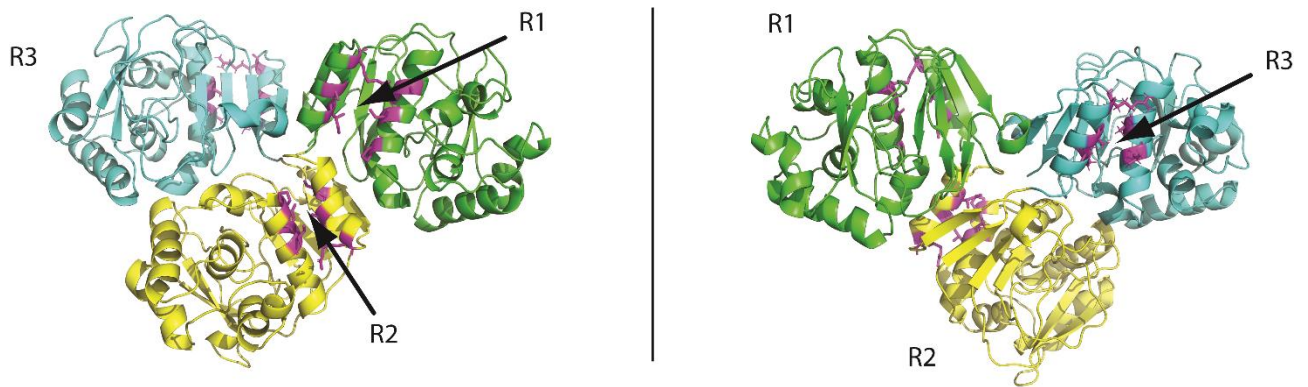


**Figure S5.** Model of CDCA1 full length [1]. Two views rotated by 180° around the y-axis are displayed. R1, R2 and R3 repeats are shown in green, yellow and cyan, respectively. Tunnel openings are indicated by arrows and their lining residues are highlighted in magenta.



**Figure S6.** Tunnel identified in CS<sub>2</sub> hydrolase from *Acidianus* A1-3 (pdb code 3TEN) [2] using CAVER [3]. The protein is shown as yellow cartoon and the long hydrophobic tunnel as red spheres. Zinc ion is displayed as a grey sphere.

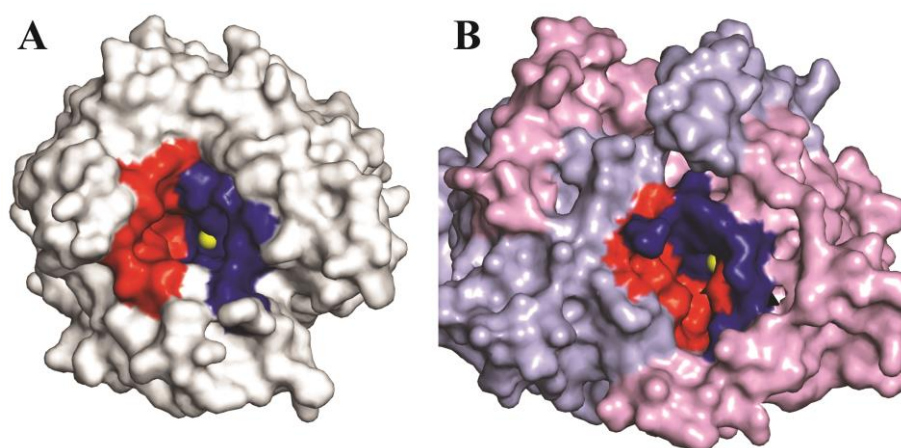


**Figure S7.** Solvent accessible surface of (A) hCA II (PDB code 1CA2) [4] and (B) the  $\beta$ -CA Nce103 from *Saccharomyces cerevisiae* (PDB code 3EYX) [5]. Putative CO<sub>2</sub> access routes are highlighted in red (hydrophobic region), blue (hydrophilic region). The catalytic zinc ion is showed as a yellow sphere.  $\beta$ -CA dimer chains A and B are reported in pink and light blue, respectively.



**Table S1.** Data collection and refinement statistics.

	<b>Zn-R3</b>	<b>Zn-R3/CO<sub>2</sub></b>
<b>Crystal parameters</b>		
Space group	C2	C2
a (Å)	117.8	119.6
b (Å)	62.5	62.7
c (Å)	75.4	75.0
β (°)	120.1	119.8
<b>Data collection statistics</b>		
Resolution (Å)	50.0-1.98 (2.02-1.98)	50.0-1.60 (1.63-1.60)
Temperature (K)	100	100
Total reflections	147785	710837
Unique reflections	31341	61450
Completeness (%)	95.2 (75.7)	97.0 (78.0)
<I>/<σ(I)>	13.3 (2.1)	35.8 (3.9)
Redundancy (%)	4.7 (2.7)	11.6 (7.1)
R <sub>merge</sub> <sup>a</sup>	0.093 (0.454)	0.066 (0.443)
R <sub>meas</sub> <sup>a</sup>	0.103 (0.555)	0.068 (0.474)
R <sub>pim</sub> <sup>a</sup>	0.043 (0.311)	0.019 (0.162)
CC1/2 <sup>b</sup>	0.996 (0.794)	0.999 (0.949)
<b>Refinement statistics</b>		
Resolution (Å)	33.24-1.98	50.0-1.60
R <sub>work</sub> <sup>c</sup> (%)	20.8	21.5
R <sub>free</sub> <sup>c</sup> (%)	24.3	24.6
r.m.s.d. from ideal geometry:		
Bond lengths (Å)	0.009	0.009
Bond angles (°)	1.5	1.5
Number of protein atoms	3188	3183
Number of ligand atoms		6
Number of water molecules	152	171
Average B factor (Å <sup>2</sup> )		
All atoms	28.1	26.4
Protein atoms	28.0	26.1
Ligand atoms		32.8
Water molecules	29.8	30.5
<b>PDB Code</b>	<b>7BEZ</b>	<b>7BF0</b>

<sup>a</sup>R<sub>merge</sub> =  $\frac{\sum_{hkl} \sum_i |I_i(hkl) - \langle I(hkl) \rangle|}{\sum_{hkl} \sum_i I_i(hkl)}$ ; R<sub>meas</sub> =  $\frac{\sum_{hkl} \{n(hkl)/[n(hkl)-1]\}^{1/2} \sum_i |I_i(hkl) - \langle I(hkl) \rangle|}{\sum_{hkl} \sum_i I_i(hkl)}$ ; R<sub>pim</sub> =  $\frac{\sum_{hkl} \{1/[n(hkl)-1]\}^{1/2} \sum_i |I_i(hkl) - \langle I(hkl) \rangle|}{\sum_{hkl} \sum_i I_i(hkl)}$ , where I<sub>i</sub>(hkl) is the intensity of an observation and <I(hkl)> is the mean value for its unique reflection; summations are over all “n” reflections.

<sup>b</sup>CC1/2 =  $[\sum_i (a_i - \langle a \rangle) / \sum_i (b_i - \langle b \rangle)] / [\sum_i (a_i - \langle a \rangle)^2 / \sum_i (b_i - \langle b \rangle)^2]^{1/2}$ ; where a<sub>i</sub> and b<sub>i</sub> are the intensities of unique reflections merged across the observations randomly assigned to subsets A and B, respectively, and <a> and <b> are their averages.

<sup>c</sup>R<sub>factor</sub> =  $\frac{\sum_h |F_o(h) - F_c(h)|}{\sum_h |F_o(h)|}$ , where F<sub>o</sub> and F<sub>c</sub> are the observed and calculated structure-factor amplitudes, respectively. R<sub>free</sub> was calculated with 4.1% of the data excluded from the refinement.

**Table S2.** Tunnel residues interacting with CO<sub>2</sub> into the main pockets (**1\***, **2\***, **3\***) detected along the migration pathway.

Pocket <b>1*</b>	Pocket <b>2*</b>	Pocket <b>3*</b>
Val628, Val584, Ala624 Val474, Phe603	Trp448, Val584, Ile586, Val605, Ala624, Ala625, Ala637	Ile439, Ala442, Leu443, Arg446, Leu620, Val618, Val622

## References

- [1] Alterio V, Langella E, Viparelli F, Vullo D, Ascione G, Dathan NA, et al. Structural and inhibition insights into carbonic anhydrase CDCA1 from the marine diatom *Thalassiosira weissflogii*. *Biochimie* 2012;94:1232-1241.
- [2] Smeulders MJ, Pol A, Venselaar H, Barends TR, Hermans J, Jetten MS, et al. Bacterial CS<sub>2</sub> hydrolases from *Acidithiobacillus thiooxidans* strains are homologous to the archaeal catenane CS<sub>2</sub> hydrolase. *J Bacteriol* 2013;195:4046-4056.
- [3] Chovancova E, Pavelka A, Benes P, Strnad O, Brezovsky J, Kozlikova B, et al. CAVER 3.0: a tool for the analysis of transport pathways in dynamic protein structures. *PLoS Comput Biol* 2012;8:e1002708.
- [4] Eriksson AE, Jones TA, Liljas A. Refined structure of human carbonic anhydrase II at 2.0 Å resolution. *Proteins* 1988;4:274-282.
- [5] Teng YB, Jiang YL, He YX, He WW, Lian FM, Chen Y, et al. Structural insights into the substrate tunnel of *Saccharomyces cerevisiae* carbonic anhydrase Nce103. *BMC Struct Biol* 2009;9:67.